Antimicrobial microneedle patch for treating deep cutaneous fungal infection

Zan, Ping; Than, Aung; Duong, Phan Khanh; Song, Juha; Xu, Chuanhui; Chen, Peng

2019

Zan, P., Than, A., Duong, P. K., Song, J., Xu, C. & Chen, P. (2019). Antimicrobial microneedle patch for treating deep cutaneous fungal infection. Advanced Therapeutics, 2(10), 1900064-. https://dx.doi.org/10.1002/adtp.201900064

https://hdl.handle.net/10356/147531

https://doi.org/10.1002/adtp.201900064

Antimicrobial Microneedle Patch for Treating Deep Cutaneous Fungal Infection

Ping Zan[1], *Aung Than*[1], *Phan Khanh Duong*[1], *Juha Song*[1], *Chuanhui Xu*[2] *and Peng Chen*[1]*

[1]School of Chemical and Biomedical Engineering, Nanyang Technological University, 70 Nanyang Drive, Singapore 637457

[2]Department of Rheumatology, Allergy and Immunology, Tan Tock Seng Hospital, Singapore 308433

Keywords: antimicrobial polymer, microneedle, skin infection, fungal infection

Abstract

Subcutaneous fungal infection is often difficult to be treated by the conventional topical application or oral intake of antifungal agents because of low drug bioavailability to the infection site, lack of sustained therapeutic effect, and development of drug resistance. Here, we report a new strategy using polymeric microneedle (MN) patch to overcome the skin barrier. MN is made of biocompatible and biodegradable chitosan-polyethylenimine copolymer which possesses antimicrobial property immune to drug resistance and allows sustained drug release. Using a fungal infection mouse model, we demonstrate that MN patches encapsulated with antifungal agent amphotericin B offer outstanding treatment effectiveness, which is attributable to the high bioavailability of therapeutics and synergistic actions of antifungal polymer and drug.

1. Introduction

Skin fungal infection (mycosis) affects 20-25% of the population worldwide.[1] Deep cutaneous mycoses are difficult to treat and may cause serious consequences even morbidity, particularly to immunosuppressed people.[2] AIDS and cancer patients whose immune systems are impaired are particularly prone to serious fungal infection.[2c, 3] In general, fungi are considered ~~is~~ more difficult to be killed than bacteria because, unlike bacteria, they are not only eukaryotic cells with multi-organelles ~~as well as~~but also contain thick and rigid cell walls which are resistant to lysis by the innate immune response.[4]

~~Conventionally,~~Skin mycoses are currently treated with topical creams, ointments, gels, and lotions containing antifungal drugs (e.g., fluconazole and amphotericin B).[5] Fungi on the skin surface are able to migrate through the epidermis and dermis to the subcutaneous tissue.~~Fungi are able to migrate from skin surface into deeper layers of epidermis, dermis even subcutaneous tissues.~~[6] Although current topical formulations are effective to treat superficial fungal infection, they are not effective against ~~to~~ deep cutaneous fungal infection because of poor drug penetration ~~across~~ through the stratum corneum.[5a, 7] Incomplete elimination of fungi in chronic infection can lead to the development of multidrug-resistant fungi, and further ~~If fungi are not eliminated completely in sustained infection, antifungal resistance will be developed and~~ spreading of fungi~~infection~~ could be ~~life~~ life-threatening.[8]

As compared ~~with~~ to topical applications, oral intake of antifungal drugs shows better therapeutic effect towards deep cutaneous fungal infection. However, systemic administration of drug can cause adverse side effects ~~But such systemic drug administration often causes side effects~~ (e.g., hepatoxicity and teratogenicity) due to non-specific drug accumulation in non-targeted tissues.[9] On the other hand, surgical interventions ~~Surgical measures~~ (e.g., debridement) are expensive and painful. And it is not easy to completely remove the infected tissues, and the surgical wound left is ~~and the left wound sites are~~ vulnerable to be infected again.[10] Therefore, it is imperative to develop new highly effective, safe, and patient-friendly methods to combat mycoses.

Transdermal drug delivery based on microneedles (MNs), which is a minimally-invasive and pain-free technology capable of helping therapeutics to overcome the stratum corneum barrier, has been employed to treat various diseases including skin cancers, skin bacterial infection, diabetes, obesity, eye diseases, etc.[11] MNs are usually made of degradable polymers to encapsulate therapeutics and control release kinetics.[12]

Antimicrobial polymers have attracted increasing attention due to their abilities to kill drug-resistant microbes by ~~for their ability to against resistance microbes by~~ disrupting their

membranes.[13] Therefore, MNs made of antimicrobial polymers shall be promising for the treatment of skin infections. Several studies have been paid seeking the development of novel antimicrobial polymers.[14] Besides, studies also reported the use of antimicrobial polymers and drug combinations to counteract drug resistance.[15] Chitosan is a natural, biocompatible, and biodegradable cationic polysaccharide known for its intrinsic antimicrobial ability.[16] It has ~~also~~ been used as drug carriers for sustained drug release.[17] Branched polyethylenimine (PEI) with rich protonated amines at physiological pH can also electrostatically interact with negatively charged microbial surface to induce membrane disruption and cell lysis.[18] Although PEI has high antimicrobial activity, it is cytotoxic to animal cells.~~Although with high antimicrobial potency, PEI also induce cytotoxicity to animal cells.~~[19] Here, we for the first time use ~~In this contribution, we for the first time synthesize~~ chitosan-polyethylenimine (CP) copolymer as the antimicrobial polymer ~~and use it~~ to fabricate MN patches to treat deep cutaneous fungal infection (**Figure 1**). ~~Comparing~~ Compared to conventional topical drug application, such microneedle approach provides ~~much~~ superior therapeutic effectiveness owing to the localized drug delivery, high drug bioavailability, and sustained synergistic antifungal effects from both CP and encapsulated drug (amphotericin B) ~~and high localized drug bioavailability~~.

2. Results

2.1. Characterization of chitosan-polyethylenimine (CP) copolymer

CP copolymer was firstly synthesized by an imine reaction between chitosan and low molecular weight PEI. As shown in ^{1}H NMR spectra (Figure S1a, Supporting Information), the areas of proton peaks from CP (3.299-2.655 ppm) are increased as compared ~~with~~ to ~~that~~ those from chitosan, demonstrating that chitosan and PEI ~~is~~ are successfully conjugated.[20] Consistently, zeta potential of CP copolymer became~~becomes~~ more positive ~~after conjugation of PEI~~ (Figure S1b, Supporting Information). Unlike PEI, both ~~**Figure 2**a~~ chitosan (C) and ~~demonstrates that~~ CP copolymer~~, just like chitosan (C) but in contrast to PEI, doesn't exert obvious cytotoxicity~~

are highly biocompatible to human cells ~~-~~even at a high concentration (500 μg mL^{-1}) (**Figure 2**a). ~~Fungus~~ Fungi with drug-resistance~~ant~~ (*Candida albicans*) ~~was~~ were used as the model strain in our study. Based on the light absorption of microbial culture solution at 600 nm ~~(Figure 2b)~~, it was observed that MIC (minimum inhibitory concentration to inhibit 90% growth of micro~~-~~organism) of CP (140 μg mL^{-1}) is much lower than those~~at~~ of anti~~-~~fungal agent fluconazole (460 μg mL^{-1}) and chitosan (340 μg mL^{-1}) (Figure 2b). Although antifungal agent amphotericin B is more potent than CP, its conventional administration is problematic. Together with CP (100 μg mL^{-1}), MIC of amphotericin B can be lowered from 23 to 10 μg mL^{-1}. Similarly, addition of CP significantly reduces MIC of fluconazole to 27 μg mL^{-1}. These results testify the synergy between the copolymer and drugs. In addition, CP also exhibits antimicrobial ability to bacteria including *Staphylococcus aureus (S. aureus)*, *Methicillin-resistant Staphylococcus aureus (MRSA)* and *Bacillus*. The antimicrobial ability of CP against bacteria (Figure S2, Supporting Information) and ~~fungus~~ fungi (Figure 2c) was further confirmed by fluorescence-~~staining~~ based live/dead analysis. As seen from Figure 2c and Figure S3 (Supporting Information), the surface of ~~fungus~~ fungi became porous after CP treatment, making ~~fungus~~ fungi more susceptible to the antifungal agents.

2.2. Fabrication and characterization of drug-loaded MNs

Because of the good biocompatibility and antimicrobial ability of chitosan-PEI copolymer, we use it to fabricate antifungal MN patches by a simple micromolding method. Hyaluronic acid (HA) with low molecular weight was used to make the supporting substrate, which quickly separates from the MNs as the drawn interstitial fluid dissolves the interfacial HA molecules and thus can be removed soon after MN insertion.[11c] The MN patch consists of 10 × 10 array of sharp-pointed pyramidal needles with the height of ~950 μm and base width of ~250 μm (**Figure 3**a and 3b). The mechanical strength of MN was analyzed by compression test. MNs did not break even with a displacement of 400 μm, with the mechanical force of 0.60 N/needle which is strong enough to penetrate into the skin (Figure 3c). To confirm this, Cy5 dye loaded

CP MN patches were applied onto the fresh porcine skin. After insertion for 2 min, HA supporting substrate was removed, leaving an array of blue spots that cannot be washed away (Figure 3d). It indicates that all MNs were successfully and fully inserted.

Antifungal drug amphotericin B (AB, 10% w/w) was loaded into CP MNs for synergistically enhanced potency. As shown in Figure 3c, drug loading did not significantly compromise the mechanical strength of MNs (~0.55 N/needle). Histological examination of the pork porcine skin with embeddedafter insertion of CP/AB MNs reveals the penetration depth of ~400 µm, indicating that MNs can penetrate across the epidermis (50-150 µm thick) and reach the dermal layer (Figure 3e).[21] However, polymeric matrixes of MNs were not seen in the histological section, likely due to being removed during the tissue processing, cryo-sectioning, and staining processes.[21] In physiological buffer solution, CP/AB MNs became hydrogel (pH ~7), which was decomposed completely in within 6 days, gradually releasing CP molecules into the solution (Figure S4, Supporting Information). No obvious pH changes in both CP/AB hydrogel and the buffer solution were observed during in vitro releasing process (both of pH are ~7) (Figure S5, Supporting Information). As human skin interstitial fluid has a good buffering system, with a tight pH range of 7.2 to 7.4,[22] there will be no changes in the pH of the hydrogel and the environment during drug release in vivo. In addition, it was found that CP/AB hydrogel and drug release did not affect cell viability and motility (cell motility assay was used to assess cell function) (Figure S6 and S7, Supporting Information), indicating that CP/AB MNs and drug release are not harmful to the human skin.

Next, the in vitro drug release profiles were investigated by monitoring the release of Cy5 encapsulated infrom CP MNs from in agarose hydrogel as the artificial skin (Figure 3f and 3g). Swelling of MNs and a burst release of dye molecules was were observed immediately after insertion (Figure 3f). Although most of Cy5 molecules were distributed throughout the agarose hydrogel after 24 h, bright fluorescence signals were still observed in the MN tips, After 24 h, most dyes were distributed in agarose hydrogel but still with bright fluorescence signals in the

~~MN tips,~~ demonstrating that the release is sustained (Figure 3g). Further~~more~~, in vivo release of Cy5-loaded CP MN~~s~~ was evaluated based on the change~~s~~ of fluorescence signal as the dye molecules were released and diffuse~~d~~ away from the application site~~s~~. As shown in Figure 3h and 3i, the release lasted over 72 h with a time constant of 27.03 h.

2.3. Drug-loaded CP MNs for treating deep cutaneous fungal infection

In vivo therapeutic effects of AB-loaded CP MNs on subcutaneous fungal infections ~~was~~ were investigated ~~in~~ using a *Candida albicans (C. albicans)*-inoculated mouse model.[23] Mice were injected intradermally with *C. albicans* suspension and randomly separated into six groups with seven in each. Prominent nodule appeared below the skin after 1 d, indicating that the mice were suffered from fungal infection.

Nodules of the non-treated mice (control) as well as mice treated with HA MNs (MNs made of HA) ~~two mouse groups without any treatment or treated with polymeric equipped with MNs patch made of hyaluronic acid (HA MNs)~~ grew over time (**Figure 4**a and 4b). On the other hand, treatment with CP MNs suppressed the nodule growth, demonstrating the antimicrobial effects of CP copolymer. In contrast, CP MNs loaded with AB largely eliminated the nodule, indicating the synergistic effects of antimicrobial polymer and drug (Figure 4a and 4b, Figure S9, Supporting Information). In comparison, topical application of cream containing the same amount of CP copolymer and AB was not able to inhibit the nodule growth because of the poor skin penetration, and hence low bioavailability of these antimicrobial agents. HA MNs loaded with AB ~~was~~ were not able to significantly inhibit nodule growth over time, owing to the fast release and clearance of the drugs.[11e]

At day 6, the mice were euthanized and nodules beneath the infected skin were measured~~,~~. As shown in Figure 4c and 4d, ~~confirming that~~ CP/AB MN~~s~~ offer~~s~~ the best treatment outcome ~~(Figure 4c and 4d)~~. Histological analyses show that the skin thickness and morphology after CP/AB MN treatment~~s~~ ~~is~~ are nearly identical to the healthy skin whereas infection and swelling remain prominent after other treatments (Figure 4e and 4f). It is noted that CP MN treatment is

much better than HA/MN, HA/AB MN, and CP/AB cream treatments because the MNs themselves have good antifungal property and are able to overcome the barrier of stratum corneum. It is inferior to CP/AB MN because of the absence of synergistic action of antifungal polymer and drug. Periodic acid Schiff (PAS) staining targeting on high content of polysaccharides in the cell wall was used to specifically label fungi (Figure 4g).[24] In contrast to other treatments, only CP/AB MN treated skin shows a trace amount of fungi similar to that in healthy skin. The infected skin tissues treated by CP/AB MNs are~~is~~ still slightly thicker than the healthy skin, likely due to the lasting inflammation.

3. Discussion and Conclusion

Effective transdermal drug delivery to treat subcutaneous mycoses remains challenging due to the skin barrier and drug-resistance.[5a, 25] To tackle these issues, we demonstrate a transdermal patch equipped with an array of drug-encapsulated microneedles (MNs) made by antimicrobial polymers. MNs can be self-implanted subcutaneously and serve as micro-reservoirs to locally release antifungal effect sustainably in desired kinetics without causing side effects. We show that chitosan-polyethylenimine (CP) copolymer is biocompatible and has potent antifungal and antibacterial ability. MNs made of ~~it~~ CP copolymer ~~has~~ have sufficient mechanical strength for the skin penetration and provide sustained antimicrobial effect ~~with dissolving time~~ over several days which is comparable to the skin turn-over time of mouse. In addition, the synergistic effects of antifungal polymer and drug are demonstrated both in vitro and in vivo. Finally, using a *C. albicans*-inoculated mouse model, it is found that this microneedle approach is superior to the conventional cream application. The outstanding effectiveness is attributable to high and localized bioavailability of therapeutics by overcoming the barrier of stratum corneum, synergistic combination of antifungal polymer and drug, and sustained therapeutic effect.

Conventional antimicrobial agents are often plagued by the development of drug-resistance because of the molecular and genetic adaptation of microbes and biofilm formation.[25] In

contrast, antimicrobial polymers offer high antimicrobial activity without inducing drug resistance because they act by physically disrupting microbial membranes.[26]

Apart from subcutaneous candidiasis, other deep cutaneous mycoses, such as mycetoma, and chromoblastomycosis could be effectively treated by our strategy.[27] It is also possible to be used for treating fungal eye infections such as keratitis.[11d] As CP copolymer is also active for killing bacteria (Figure S2, Supporting Information), our MN patch is also promising for treating subcutaneous bacterial infections, such as cellulitis.[28] Various types of antimicrobial polymers have been identified or synthesized, for examples, polymers containing quaternary nitrogen atoms, guanidine, phospho and sulfo derivatives.[29] In addition to antimicrobial drugs, antimicrobial peptides, enzymes or nanoparticles may also be loaded into MNs.[30] These abundant choices make the microneedle approach potentially applicable to many diseases. In addition, the minimally invasive microneedle approach is suitable for convenient self-administration at home.

4. Experimental Section

Materials. Chitosan (75-85% deacetylated, viscosity 300 mPa·s), branched ~~Polyethylenimine~~ polyethylenimine (PEI) (average M_w 800 Da), fluconazole, amphotericin B, acetic acid, sodium hydroxide (NaOH), 1,1′-carbonyldiimidazole (CDI) were purchased from Sigma-Aldrich. Sodium hyaluronic acid (HA) (<10 kDa) was purchased from Bloomage Freda Biopharm. Dulbecco's modified eagle medium (DMEM), fetal bovine serum (FBS), penicillin-streptomycin (10,000 U ml^{-1}), and trypsin-EDTA (0.5 %, 10 X) were obtained from Gibco Life Technologies. Phosphate buffered saline (PBS, 1X) was purchased from Lonza. All reagents are of analytical grade and used without further purification.

Synthesis and ~~characterisation~~ characterization of CP copolymer. The c~~C~~opolymer was prepared according to the previously reported method for gene delivery.[20a] Briefly, 1 g of chitosan was dissolved into 100 mL of DI water containing 0.3% (v/v) acetic acid, followed by overnight stirring and titrating pH to 7.0 by NaOH (1 M). Subsequently, CDI was added into

the solution with a molar ratio of 2:1 (CDI:amines in chitosan), following by stirring for 1 h. PEI was then added dropwise under continuous stirring with a molar ratio of 2:1 (PEI:amines in chitosan). Polymerization reaction continued overnight at room temperature. The resulting product was dialyzed against water for another 48 h to remove extra free PEI. Lastly, CP powder was obtained through lyophilization and characterized by ^{1}H NMR spectroscopy (Bruker Avance II 300MHz NMR). The zeta potential was determined by a Malvern Nano-ZS Zeta Sizer machine (Malvern Instruments). The pH was measured by a pH meter (SevenCompact pH meter S210).

Fabrication of drug-loaded MN patches. MN patches were fabricated by a micromolding method. Specifically, poly(dimethylsiloxane) (PDMS) mold was firstly prepared via pouring the mixture of PDMS and curing agent (weight ratio of 10:1) into a stainless-steel master structure, which consists of 10 × 10 array~~s~~ of sharp-pointed pyramidal MNs with a base width of 300 μm, height of 1000 μm, and interspacing of 700 μm. Subsequently, PDMS mold was degassed and dried in a vacuum oven at 70 °C for 1 h. CP powders were dissolved into an aqueous solution with acetic acid (1%, v/v). The CP solution (20 mg mL^{-1}) was then dialyzed (MWCO: 10 kDa) against DI water to remove extra acetic acid until reaching pH 6. After that, CP solution was evaporated in an oven at 37 °C until reaching the final concentration of 5 wt%. This glutinous CP solution was collected for CP -MN patch fabrication. For drug loading, ~~fluconazole (F) or~~ amphotericin B (AB) was firstly dissolved into DMSO (40 mg/mL). Then 125 μL of the drug solution was vortexed with CP solution (875 μL) overnight before fabrication of drug-loaded CP -MN patch. To make MN patches, concentrated CP and CP+AB solution ~~was~~ were filled into PDMS mold by centrifugation (4000 rpm, 10 min). After being left overnight for drying, HA solution (<10 kDa, 500 mg mL^{-1}) was added onto the mold and centrifuged for the supporting substrate of MN patch. Finally, the MN patch was carefully detached from the mold after overnight drying. The residual acetic acid left in MNs was further

removed during the drying process due to its highly volatile nature. The pH of CP/AB hydrogel after immersion of CP/AB MNs into the buffer solution is around 7.

Mechanical test and in vitro penetration test. The mechanical strength of MNs was analyzed by an Instron 5543 Tensile Meter. A continuous force was administered to the tips of MNs which ~~was~~ were placed upwards on a flat stainless-steel probe, until a displacement of 400 μm was achieved at a constant speed of 0.5 mm/min.

To evaluate the skin penetration ability, MN patches were applied vertically onto the fresh porcine skin for ~2 mins before the HA substrate was removed~~, leaving MNs embedded in the skin~~. The skin was then excised, fixed with 10% f~~ormaldehy~~formalin~~de~~ solution for 1 day, and cryoprotected with 30% sucrose solution for 2 days. After being frozen sectioned (10 μm thick) by a CM1950 cryostat (Leica Microsystem), the slides were stained with haematoxylin and eosin (H&E), and the images were obtained by a digital microscope (Leica DVM6).

In vitro and in vivo drug release. To determine in vitro drug release profiles of CP MN, Cy5 was loaded in MNs and its release was imaged by confocal microscope (LSM800, Carl Zeiss) after MNs being inserted into agarose hydrogel. Seven to eight-week old male C57BL/6J mice were used to examine in vivo release profiles of Cy5 dye from CP MNs. After applying the MN patch, the mice were imaged at different times (0 h, 3 h, 24 h, 48 h, and 72 h) by an in vivo imaging system (IVIS Spectrum, Perkin Elmer).

Cytotoxicity and cell motility assays. Cytotoxicity of CP copolymer was evaluated using an AlamarBlue cell viability assay (ThermoFisher). Briefly, human Hela cells (~~NIH/3T3 cell,~~ ATCC) were incubated in culture medium (DMEM with 10% FBS) overnight, followed by the exposure to CP copolymer with different concentrations for 24 h. In addition, to investigate the impact of CP/AB MNs on the cell viability during drug release process, human Hela cells were also exposed to CP/AB MNs (~500 μg) for one day and three days respectively. After that, cells were washed by PBS and incubated in culture medium together with 10% AlamarBlue for 2–3

h at 37 °C. Finally, the fluorescence intensity of AlamarBlue at 590 nm under 560 nm excitation was determined using a microplate reader (SpectraMax M5, Molecular Devices).

Cell motility assay was performed as described previously.[31] Firstly, human Hela cells were incubated overnight. A straight scratch was made using a pipette tip on the confluent cell monolayer. After removing the floating cells, the remaining cells were exposed to CP/AB MNs (~500 μg). Bright-field images were taken in the rigion along the scratch at day0, day1 and day2 using a digital microscope (Leica DVM6), and the scratch distances were measured using ImageJ.

Minimum inhibitory concentration (MIC) test. Candida albicans (*C. albicans*) were incubated overnight in YPD broth (10 g of yeast extraction, 20 g of peptone, and 20 g of dextran dissolved in 1 L of deionized water) at 30 °C in a shaking incubator. They were then diluted to 10^4 to 10^5 colony forming units (CFUs)/mL in PBS. Different concentrations of 100 μL of CP solution in YPD broth ~~was~~ were added into a 96-well microplate, followed by adding 100 μL of fungi suspension. Subsequently, the plates were put in a shaker incubator at 30 °C for 18-24 h. Finally, a microplate reader (SpectraMax M5, Molecular Devices) was used to measure the absorbance at 600 nm of the 96-well plate. The percentage of microbial inhibitory rate was calculated according to Equation 1.

(Equation) $$\text{Inhibition rate (\%)} = \frac{\text{OD of normal microbial growth-OD of inhibited microbial growth}}{\text{OD of normal microbial growth}} \times 100 \quad (1)$$

OD of inhibited microbial growth was obtained by subtracting OD of polymer solution.

Live/dead assay. 100 μL of fungi or bacteria suspension (5×10^8 CFUs/mL) in PBS (500 μL) with or without CP copolymer was incubated for 1 h at 30 °C (for fungi) or 37 °C (for bacteria). Then, the fungi or bacteria suspension was stained with a LIVE/DEAD Kit (L7012, Thermofisher) for another 20 min at room temperature. Finally, they were imaged with a confocal microscope.

Dermal infection mouse model. All the animal experiments were approved by Institutional Animal Care and Use Committee of Nanyang Technological University (NTU-IACUC, A18029). Firstly, *C. albicans* (5 x 10^6 CFUs/mL) were cultured at 37 °C with 10% FBS for 2 h in order to change the morphology of fungi from blastospores to pseudohyphae. Next, the density of fungi was adjusted to 5 x 10^6 CFUs/mL by PBS, and the suspension (50 μL) was intradermally injected into the ~~deep~~ dermis of the shaved back of each mouse. After 1d, nodules were formed on the injected region. These inoculated mice were then randomly separated into 6 groups with seven in each. One was designated as control, other five groups were treated once with CP/AB MN, CP MN, HA MN, HA/AB MN, and CP/AB cream (0.5 wt% AB in 4.5 wt% CP solution) respectively. At day1, MN patches were applied gently on the infected area. The swelling sizes (diameters) of mice skin were measured by a micro-caliper and recorded every day. At day 6, the mice were euthanized, and the deep skins were imaged and collected for histology analysis. The mice skin tissues were immersed in 10% ~~formaldehyde~~ formalin solution for 1d and subsequently dipped into 30% sucrose solution for two more days. Then, they were frozen, ~~and~~ cut into slices with 10 μm thick, and stained with periodic acid-schiff (PAS). PAS staining areas were measured by using the ImageJ software.[32]

Statistical analyses. All quantitative data ~~analyzed~~ were shown as mean ± standard deviations (SD). Statistical analysis among groups was ~~executed~~ performed using one-way analysis of variance (ANOVA) followed by Tukey's post-hoc test. Unless otherwise stated, all experiments were carried out using at least three different samples per group. A p value < 0.05 was regarded as statistically significant. Statistical analysis was performed by Prism6 software.

Supporting Information

Supporting Information is available from the Wiley Online Library or from the author.

Acknowledgements

This research is supported by Singapore Ministry of Education under its AcRF Tier 1 Grant (RG52/17). We thank Prof. Swee Hin Teoh for providing access to the imaging facility.

Conflict of Interest

The authors declare no conflict of interest.

References

[1] B. Havlickova, V. A. Czaika, M. Friedrich, *Mycoses* **2008**, *51*, 2.

[2] a) G. W. Elgart, *Semin. Cutaneous Med. Surg.* **2014**, *33*, 146; b) R. J. Hay, *Clin. Dermatol.* **2006**, *24*, 201; c) G. Garber, *Drugs* **2001**, *61*, 1.

[3] *Nat. Microbiol.* **2017**, *2*, 17120.

[4] a) B. E. de Pauw, *Mediterr. J. Hematol. Infect. Dis.* **2011**, *3*, e2011001; b) M. G. Netea, G. D. Brown, B. J. Kullberg, N. A. Gow, *Nat. Rev. Microbiol.* **2008**, *6*, 67.

[5] a) S. Verma, P. Utreja, *Asian J. Pharm.* **2019**, *14*, 117; b) T. M. Arnold, E. Dotson, G. A. Sarosi, C. A. Hage, *Proc. Am. Thorac. Soc.* **2010**, *7*, 222.

[6] A. A. Kyle, M. V. Dahl, *Am. J. Clin. Dermatol.* **2004**, *5*, 443.

[7] N. Akhtar, A. Verma, K. Pathak, *Curr. Pharm. Des.* **2015**, *21*, 2892.

[8] a) J. Wang, S. Chou, Z. Yang, Y. Yang, Z. Wang, J. Song, X. Dou, A. Shan, *J. Med. Chem.* **2018**, *61*, 3889; b) L. E. Cowen, D. Sanglard, S. J. Howard, P. D. Rogers, D. S. Perlin, *Cold Spring Harbor Perspect. Med.* **2015**, *5*, a019752.

[9] a) N. Spernovasilis, D. Kofteridis, *J. Fungi* **2018**, *4*, 133; b) L. Tuffanelli, P. B. Milburn, *J. Am. Acad. Dermatol.* **1990**, *23*, 728.

[10] T. Koga, T. Matsuda, T. Matsumoto, M. Furue, *Am. J. Clin. Dermatol.* **2003**, *4*, 537.

[11] a) J. Yang, X. Liu, Y. Fu, Y. Song, *Acta Pharm. Sin. B* **2019**, DOI: https://doi.org/10.1016/j.apsb.2019.03.007; b) J. Xu, R. Danehy, Z. Ao, H. Cai, M. Pu, A. Nusawardhana, D. Rowe-Magnus, F. Guo, *ACS Appl. Mater. Interfaces* **2019**, *11*, 14640; c) A. Than, K. Liang, S. Xu, L. Sun, H. Duan, F. Xi, C. Xu, P. Chen, *Small Methods* **2017**, *1*, 1700269; d) A. Than, C. Liu, H. Chang, P. K. Duong, C. M. G. Cheung, C. Xu, X. Wang, P. Chen, *Nat. Commun.* **2018**, *9*, 4433; e) Y. Zhang, P. Feng, J. Yu, J. Yang, J. Zhao, J. Wang, Q. Shen, Z. Gu, Adv. Ther. **2018**, *1*, 1800035; f) J. Wang, Y. Ye, J. Yu, A. R. Kahkoska, X. Zhang, C. Wang, W. Sun, R. D. Corder, Z. Chen, S. A. Khan, B. J. B, Z. Gu, *ACS Nano* **2018**, *12*, 2466; g) Y. Hao, Y. Chen, M. Lei, T. Zhang, Y. Cao, J. Peng, L. Chen, Z. Qian, Adv. Ther. **2018**, *1*, 1800008.

[12] a) W. Li, R. N. Terry, J. Tang, M. R. Feng, S. P. Schwendeman, M. R. Prausnitz, *Nat. Biomed. Eng.* **2019**, *3*, 220; b) X. Jin, D. D. Zhu, B. Z. Chen, M. Ashfaq, X. D. Guo, *Adv. Drug Delivery Rev.* **2018**, *127*, 119; c) Y. Ye, J. Yu, D. Wen, A. R. Kahkoska, Z. Gu, *Adv. Drug Delivery Rev.* **2018**, *127*, 106.

[13] a) M. Santos, A. Fonseca, P. Mendonça, R. Branco, A. Serra, P. Morais, J. Coelho, *Materials* **2016**, *9*, 599; b) W. Chin, G. Zhong, Q. Pu, C. Yang, W. Lou, P. F. De Sessions, B. Periaswamy, A. Lee, Z. C. Liang, X. Ding, *Nat. Commun.* **2018**, *9*, 917; c) B. Cao, F. Xiao, D. Xing, X. Hu, *Small* **2018**, *14*, 1802008.

[14] a) C.-K. Chen, M.-C. Lee, Z.-L. Lin, C.-A. Lee, Y.-C. Tung, C.-W. Lou, W.-C. Law, N.-T. Chen, K.-Y. A. Lin, J.-H. Lin, *Mol. Pharmaceutics* **2019**, *16*, 709; b) F. Xiao, B. Cao, C. Y. Wang, X. J. Guo, M. G. Li, D. Xing, X. L. Hu, *ACS Nano* **2019**, *13*, 1511.

[15] a) R. Namivandi-Zangeneh, Z. Sadrearhami, D. Dutta, M. Willcox, E. Wong, C. Boyer, *ACS Infect. Dis.* **2019**, DOI: https://doi.org/10.1021/acsinfecdis.9b00049; b) B. H. Hu, C. Owh, P. L. Chee, W. R. Leow, X. Liu, Y.-L. Wu, P. Z. Guo, X. J. Loh, X. D. Chen, *Chem. Soc. Rev.* **2018**, *47*, 6917.

[16] a) M. Hosseinnejad, S. M. Jafari, *Int. J. Biol. Macromol.* **2016**, *85*, 467; b) L.Y. Zheng, J.-F. Zhu, *Carbohydr. Polym.* **2003**, *54*, 527.

[17] a) M.-C. Chen, K.-Y. Lai, M.-H. Ling, C.-W. Lin, *Acta Biomater.* **2018**, *65*, 66; b) M.-C. Chen, S.-F. Huang, K.-Y. Lai, M.-H. Ling, *Biomaterials* **2013**, *34*, 3077.
[18] a) M. C. Giano, Z. Ibrahim, S. H. Medina, K. A. Sarhane, J. M. Christensen, Y. Yamada, G. Brandacher, J. P. Schneider, *Nat. Commun.* **2014**, *5*, 4095; b) N. Sahiner, S. Sagbas, M. Sahiner, R. S. Ayyala, *Carbohydr. Polym.* **2017**, *159*, 29.
[19] K. A. Gibney, I. Sovadinova, A. I. Lopez, M. Urban, Z. Ridgway, G. A. Caputo, K. Kuroda, *Macromol. Biosci.* **2012**, *12*, 1279.
[20] a) J.-Q. Gao, Q.-Q. Zhao, T.-F. Lv, W.-P. Shuai, J. Zhou, G.-P. Tang, W.-Q. Liang, Y. Tabata, Y.-L. Hu, *Int. J. Pharm.* **2010**, *387*, 286; b) H. Lu, Y. Dai, L. Lv, H. Zhao, *Plos one* **2014**, *9*, e84703.
[21] H. Chang, M. Zheng, X. Yu, A. Than, R. Z. Seeni, R. Kang, J. Tian, D. P. Khanh, L. Liu, P. Chen, *Adv. Mater.* **2017**, *29*, 1702243.
[22] D. Bruen, C. Delaney, L. Florea, D. Diamond, *Sensors* **2017**, *17*, 1866.
[23] H. R. Conti, A. R. Huppler, N. Whibley, S. L. Gaffen, *Curr. Protoc. Immunol.* **2014**, *105*, 19.6.1.
[24] a) W. Santus, F. Mingozzi, M. Vai, F. Granucci, I. Zanoni, *J. Vis. Exp.* **2018**, *136*, e57574; b) N. V. Solis, S. G. Filler, *Nat. Protoc.* **2012**, *7*, 637.
[25] L. Scorzoni, A. C. de Paula e Silva, C. M. Marcos, P. A. Assato, W. C. de Melo, H. C. de Oliveira, C. B. Costa-Orlandi, M. J. Mendes-Giannini, A. M. Fusco-Almeida, *Front. Microbiol.* **2017**, *8*, 36.
[26] a) A. Carmona-Ribeiro, L. de Melo Carrasco, *Int. J. Mol. Sci.* **2013**, *14*, 9906; b) K. Kuroda, G. A. Caputo, *Wiley Interdiscip. Rev. Nanomed. Nanobiotechnol.* **2013**, *5*, 18.
[27] K. R. Pang, J. J. Wu, D. B. Huang, S. K. Tyring, *Dermatol. Ther.* **2004**, *17*, 523.
[28] A. B. Raff, D. Kroshinsky, *JAMA* **2016**, *316*, 325.
[29] a) A. Muñoz-Bonilla, M. Fernández-García, *Prog. Polym. Sci.* **2012**, *37*, 281; b) A. Jain, L. S. Duvvuri, S. Farah, N. Beyth, A. J. Domb, W. Khan, *Adv. Healthcare Mater.* **2014**, *3*, 1969.
[30] a) E. Pazos, E. Sleep, C. M. Rubert Perez, S. S. Lee, F. Tantakitti, S. I. Stupp, *J. Am. Chem. Soc.* **2016**, *138*, 5507; b) D. M. Eby, H. R. Luckarift, G. R. Johnson, *ACS Appl. Mater. Interfaces* **2009**, *1*, 1553.
[31] S. R. Polusani, E. A. Kalmykov, A. Chandrasekhar, S. N. Zucker, B. J. Nicholson, *J. Cell Sci.* **2016**, *129*, 4399.
[32] M. Guada, R. Ganugula, M. Vadhanam, M. N. R. Kumar, *J. Pharmacol. Exp. Ther.* **2017**, *363*, 58.

Figure captions

Figure 1. Illustration of the antimicrobial MN patch for treating subcutaneous fungal infection.

Figure 2. a) The cytotoxicity study of chitosan (C), PEI, and chitosan-PEI (CP) copolymer with increasing concentration from 0 to 500 μg mL^{-1} in Hela cells . (Mean ± SD; (n=3). b) Inhibition rate of PEI, ~~chitosan (~~C~~)~~, CP, fluconazole (F), amphotericin B (AB), CP/AB and CP/F against *C. albicans* . (Mean ± SD; (n=6). c) LIVE/DEAD viability assay of *C. albicans* on without (control) or with 1 h incubation of CP at 30 °C. Dead cells are stained with red propidium iodide. Scale bar = 10 μm. Data presents as mean value, and error bars indicate SD. n represents the number of samples for each group.

Figure 3. a) SEM image of a CP/AB MN patch. Scale bar = 200 μm. b) Representative confocal fluorescence image of CP MNs loaded with Cy5. Scale bar = 200 μm. c) Mechanical

compression test of CP MN and CP/AB MN. d) Photograph of the penetration marks on porcine skin created by Cy5-loaded MN patch. Scale bar = 2 mm. e) H&E stained porcine skin after insertion of CP/AB MN. Scale bar = 250 µm. f-g) Representative confocal images of Cy5 release from CP MN in agarose hydrogel after 2 min and 24 h, respectively. Scale bar = 200 µm. h) In vivo fluorescence imaging shows the release of Cy5 from CP MN at different times. i) Quantitative in vivo release profiles of Cy5 from CP MN. (Mean ± SD; (n=6). Data presents as mean value, and error bars indicate SD. n represents the number of samples for each group.

Figure 4. a) Images of the *C. albicans* infected site on mice. b) Change of the nodule sizes (normalized to the initial size) after treatment with CP/AB MN, CP MN, HA MN, HA/AB MN patches, and CP/AB cream. Scale bar = 2 mm. c) Images of the infection sites underneath the skin. d) Size of the internal nodules after the treatments (day 6). Scale bar = 2 mm. e) PAS histological images of the normal mice skin and inoculated mice skin after the treatments (day 6). Scale bar = 250 µm. f) Skin thickness at day 6. g) PAS staining percentage vs. control. (Mean ± SD; n=7). Data presents as mean value, and error bars indicate SD. n represents the number of samples for each group. Error bars indicate SD (n=7). Statistical comparison between among groups was performed using one-way ANOVA with a Tukey post-hoc test, $^{*}p < 0.05$, $^{**}p < 0.01$, $^{***}p < 0.001$, $^{****}p < 0.0001$ versus control (no treatment on infected skin).

Figure 1.

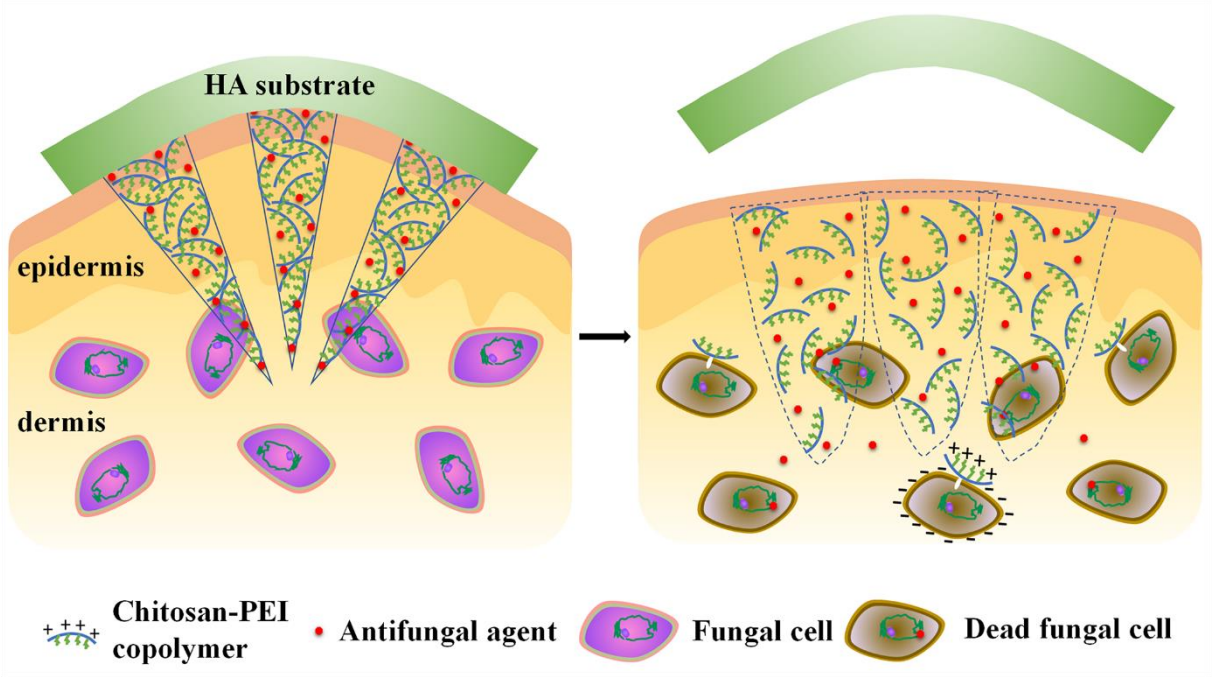
HA substrate
epidermis
dermis
Chitosan-PEI copolymer
Antifungal agent
Fungal cell
Dead fungal cell

Figure 2.

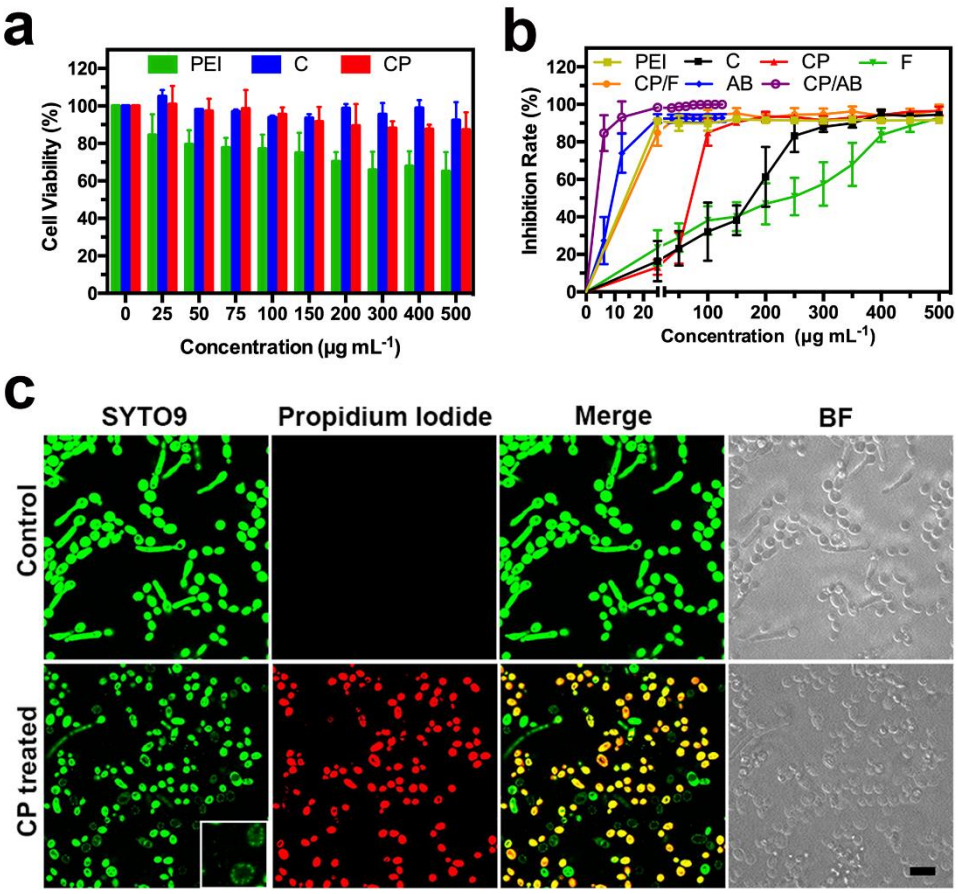
a
PEI
C
CP
Cell Viability (%)
Concentration (μg mL-1)
b
PEI
C
CP
F
CP/F
AB
CP/AB
Inhibition Rate (%)
Concentration (μg mL-1)
c
SYTO9
Propidium Iodide
Merge
BF
Control
CP treated

Figure 3.

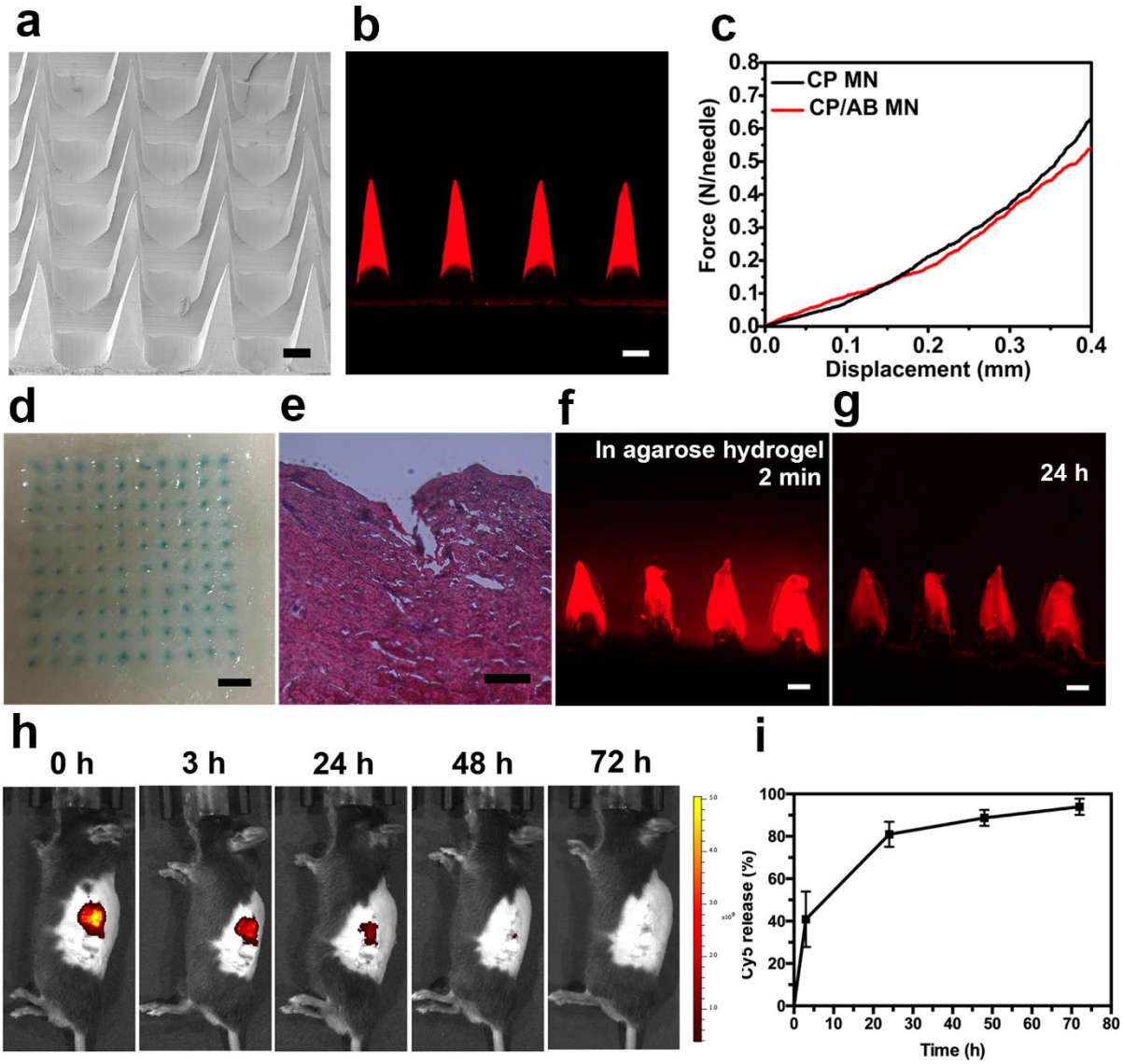
a
b
c
CP MN
CP/AB MN
Force (N/needle)
Displacement (mm)
d
e
f
In agarose hydrogel
2 min
g
24 h
h
0 h
3 h
24 h
48 h
72 h
i
Cys release (%)
Time (h)

Figure 4.

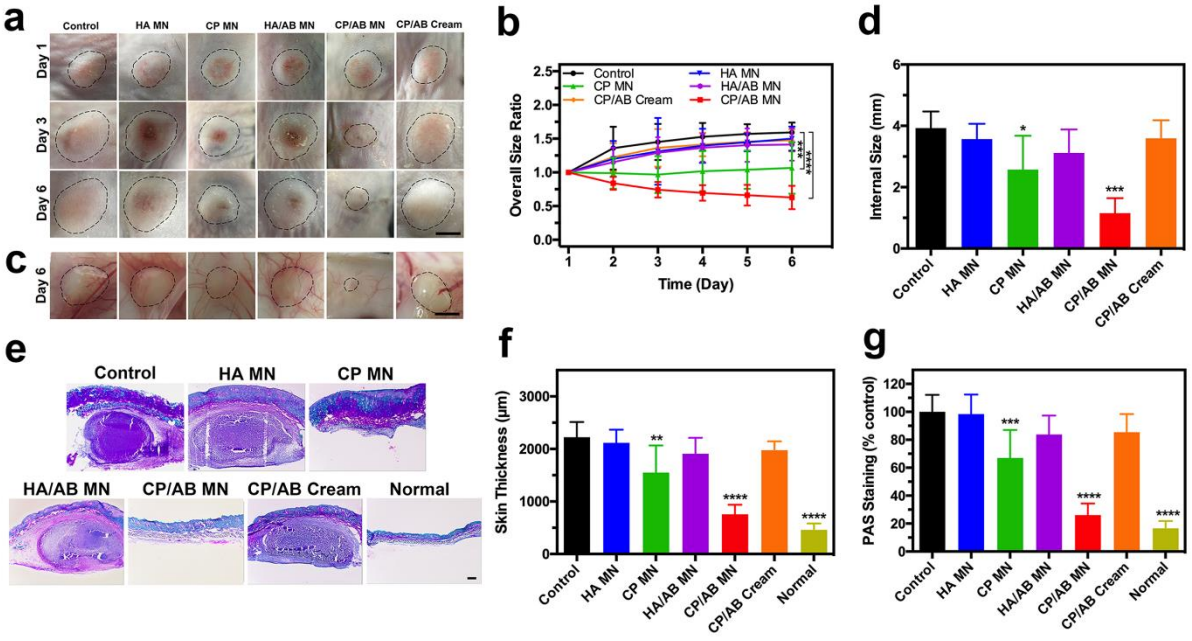
a
Control
HA MN
CP MN
HA/AB MN
CP/AB MN
CP/AB Cream
Day 1
Day 3
Day 6
c
Day 6
b
Control
CP MN
CP/AB Cream
HA MN
HA/AB MN
CP/AB MN
Overall Size Ratio
Time (Day)
d
Internal Size (mm)
e
Control
HA MN
CP MN
HA/AB MN
CP/AB MN
CP/AB Cream
Normal
f
Skin Thickness (μm)
g
PAS Staining (% control)

Table of contents

Antimicrobial Microneedle Patch for Treating Deep Cutaneous Fungal Infection

P*ing Zan*[1], *Aung Than*[1], *Phan Khanh Duong*[1], *Juha Song*[1], *Chuanhui Xu*[2] *and Peng Chen*[1]*

Keywords: antimicrobial polymer, microneedle, skin infection, fungal infection

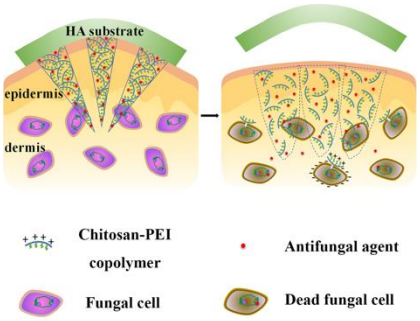

A microneedle patch made of antimicrobial polymers and encapsulated with antifungal agent is developed to treat subcutaneous fungal infection. Compared with conventional topical application, the antimicrobial patch shows superior therapeutic effects because of the enhanced drug penetration capability, sustained drug release, and synergistic therapeutic effects.

Antimicrobial Microneedle Patch for Treating Deep Cutaneous Fungal Infection

P*ing Zan*[1], *Aung Than*[1], *Phan Khanh Duong*[1], *Juha Song*[1], *Chuanhui Xu*[2] *and Peng Chen*[1]*

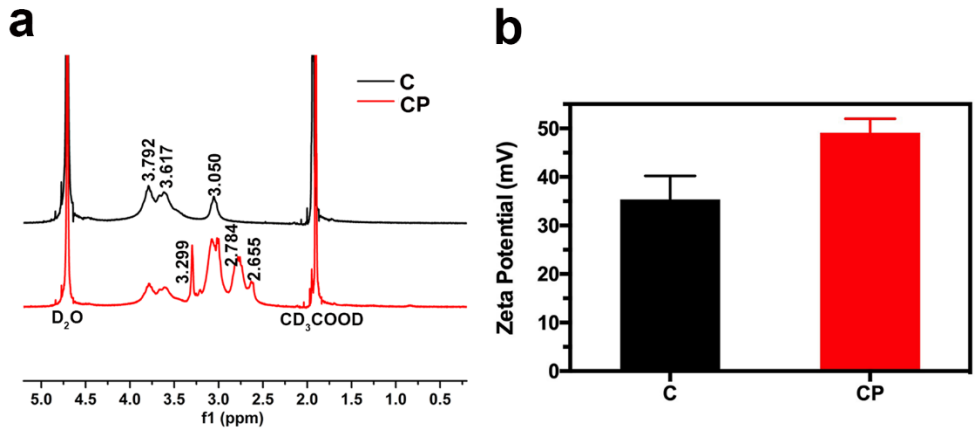

Figure S1. a) ^{1}H NMR spectra of chitosan (C) and chitosan-PEI (CP). b) Zeta potential of C and CP.

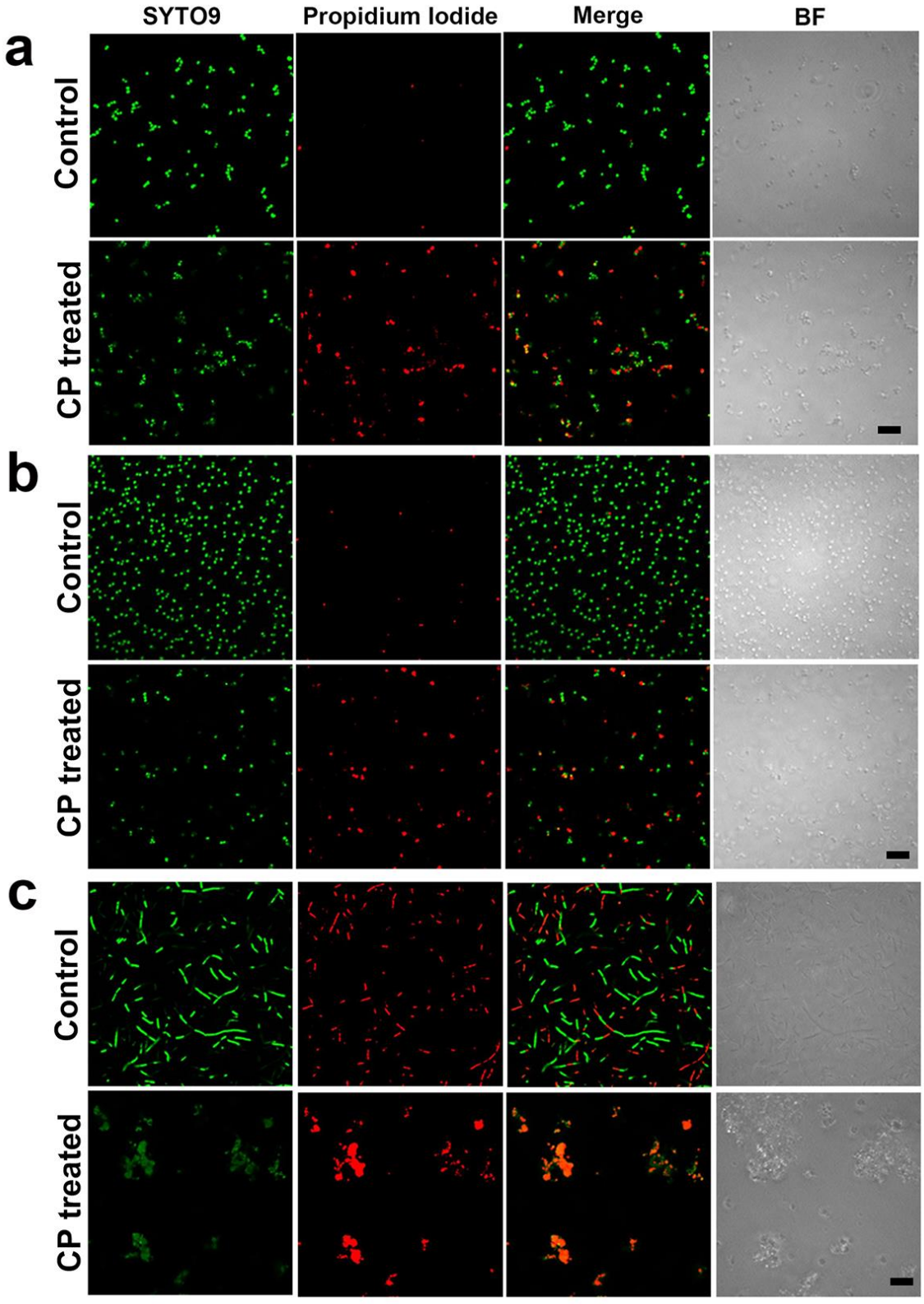

Figure S2. c) LIVE/DEAD viability assay of a) *S. aureus*, b) *MRSA* and c) *Bacillus* on without (control) or with 1 h incubation of CP at 37 °C. Dead cells are stained with red propidium iodide. Scale bar = 10 µm.

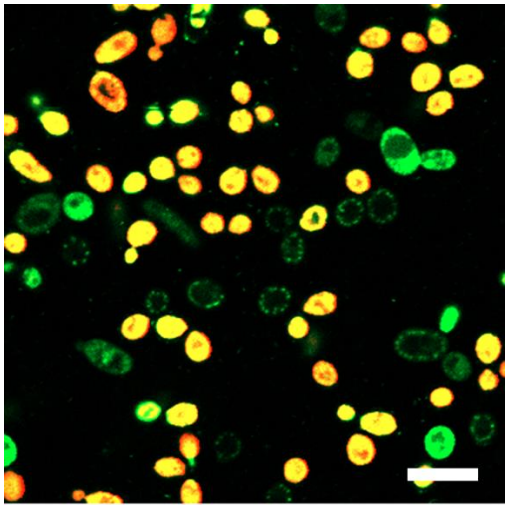

Figure S3. Confocal image of LIVE/DEAD viability assay of *C. albicans* after 1 h incubation of CP at 30 °C. Yellow color represents the merged areas of propidium iodide (red color) and SYTO9 (green color). Scale bar = 10 µm.

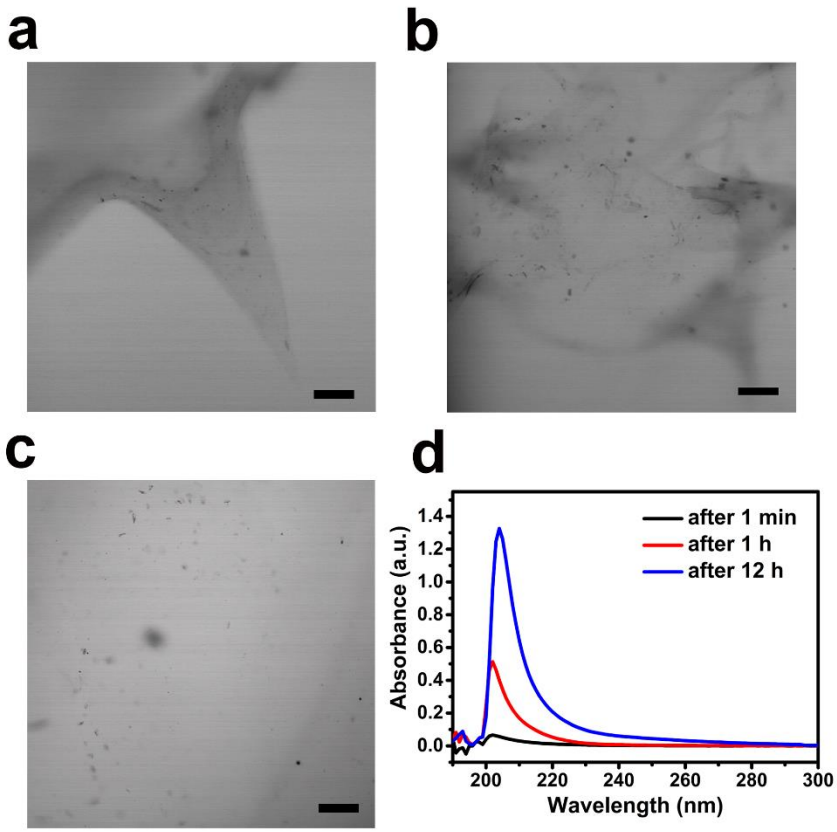

Figure S4. Bright-field images of CP MN dissolved a) immediately into PBS, b) at day 3, and c) at day 6. Scale bar = 200 µm. c) UV-vis spectrum of dispersed CP in PBS from the MNs. CP MNs were immersed into PBS for 1 min, 1 h, and 12 h. The supernatant solution after centrifuge (10000 RPM, 5 min) was analyzed by UV-vis spectrophotometry.

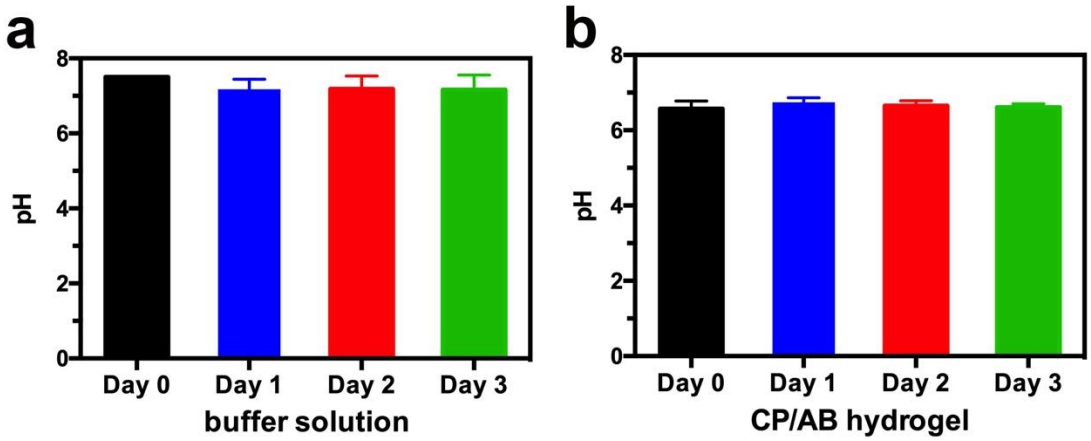

Figure S5. The pH changes of a) the buffer solution, and b) hydrogel at different days after immersing CP/AB MNs into PBS buffer solution. CP/AB MNs became hydrogel after immersing into buffer solution. The pH of the solution after centrifugation (10000 RPM, 5 min) and hydrogel was measured by the pH meter (Mean ± SD; n=3). Data presents as mean value, and error bars indicate SD. n represents the number of samples for each group. Statistical significance was calculated by one-way ANOVA, and no significant differences were found among groups.

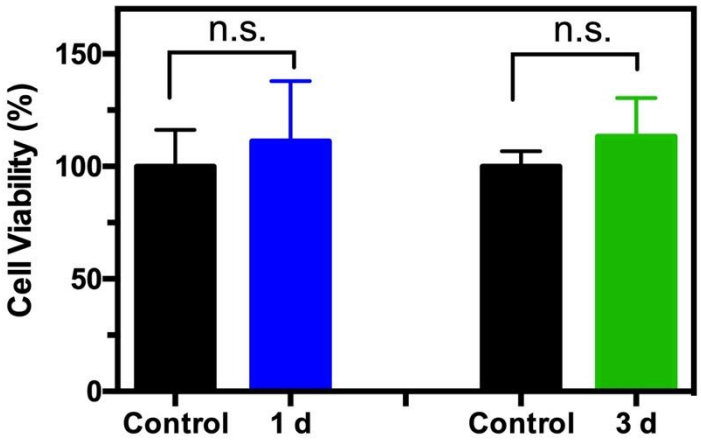

Figure S6. The cell cytotoxicity study of CP/AB MNs at different days (Mean ± SD; n=3). Data presents as mean value, and error bars indicate SD. n represents the number of samples for each group. Statistical significance was calculated by two-tailed Student's t-test, and n.s. represents no significance between indicated groups.

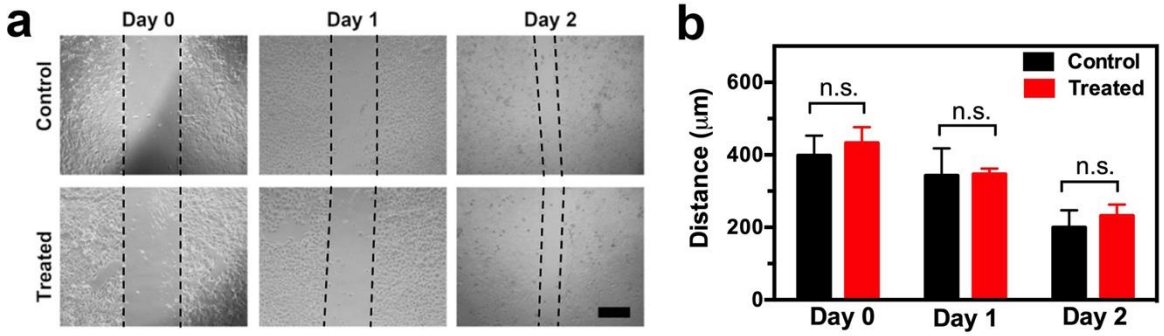

Figure S7. The cell motility study of CP/AB MNs at different days (Cell motility assay was used as a mean to analyze the cell ability) (Mean ± SD; n=3). Data presents as mean value, and error bars indicate SD. n represents the number of samples for each group. Scale bar = 250 μm. Statistical significance was calculated by two-tailed Student's t-test, and n.s. represents no significance between indicated groups.

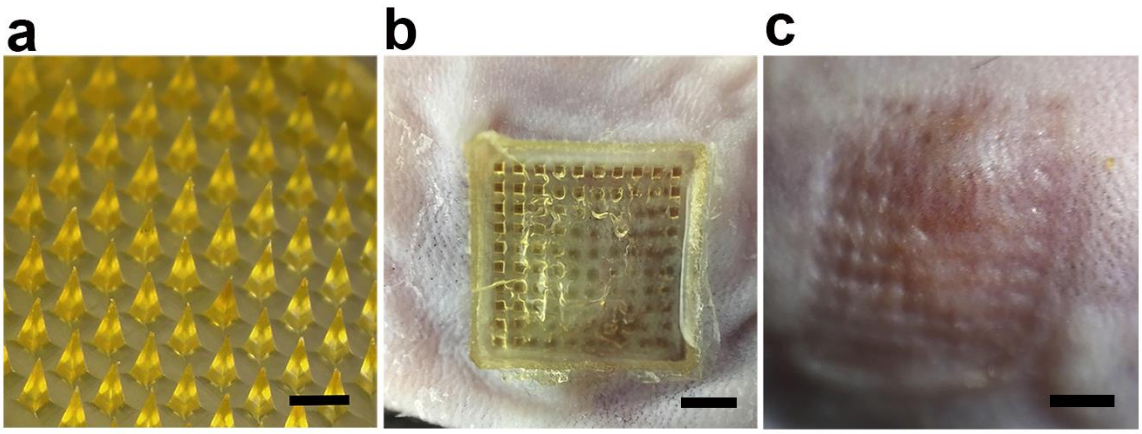

Figure S8. a) Optical images of CP/AB MN patch. Scale bar = 750 µm. Images of inoculated mice skin b) with CP/AB MN patch inserted, and c) after CP/AB MN insertion. Scale bar = 250 µm.